Communications in Mathematics and Applications
Vol. 14, No. 4, pp. 1449–1461, 2023
ISSN 0975-8607 (online); 0976-5905 (print)
Published by RGN Publications
DOI: 10.26713/cma.v14i4.2585

http://www.rgnpublications.com

***Special Issue*:**
Recent Trends in Applied and Computational Mathematics
Proceedings of the Third International Conference on Recent Trends in Applied and Computational Mathematics (ICRTACM-2022)
School of Applied Sciences, Department of Mathematics, Reva University, Bangaluru, India, 10th & 11th October, 2022
***Editors*: M. Vishu Kumar, A. Salma, B. N. Hanumagowda and U. Vijaya Chandra Kumar**

Research Article

Effect of Couple Stresses on Peristaltic Flow in a Doubly Connected Region

K. R. Rashmi[1], Indira Ramarao[1], S. Jagadeesha*[1] and K. R. Sreegowrav[2]

[1] *Department of Mathematics, Nitte Meenakshi Institute of Technology, Bengaluru, India*
[2] *Department of Mathematics, School of Applied Science, Reva University, Bengaluru, India*
***Corresponding author:** jagadeeshas31@gmail.com

Received: January 22, 2023 **Accepted:** June 16, 2023

Abstract. An eccentric annular region created by insertion of endoscope or catheter in a blood vessel is considered. A sinusoidal wave is assumed to propagate on outer wall, inner wall being rigid. A fully developed flow of couple-stress is assumed in the annular region subject to approximation of long wavelength. Analytical solution is obtained for pressure gradient and axial velocity using regular perturbation method. Average flow rate $\bar{Q}$ is fixed. The effect of azimuthal coordinate θ, couple stress parameter α and eccentricty ϵ are studied.

Keywords. Eccenticity, Couple-stress parameter, Pulsatile flow, Perturbation method, Volume flow rate

Mathematics Subject Classification (2020). 76Rxx

1. Introduction

Catheters are used extensively for measurement and inserting drugs or placing stent etc.in biological systems. Transducers are attached to catheter in order to measure pressure in the body. Similarly endoscope is inserted into digestive and urinary system for diagnostic purposes. In both situations it is necessary to study flow of both Newtonian and non-Newtonian fluids. In oesophagus, urinary tract, intestine etc. the motion of solid and semi-solid food swallowed will be due to peristalsis.

Insertion of catheter or endoscope causes reduction of area of cross section, there by reducing flow. But in case of biological system amount of oxygen, nutrients to be carried towards the tissue will be maintained. Hence flow rate has to be constant. In order to achieve this there will be an increase in pressure and in order to maintain parameters there will be a shift of catheter towards wall from the centre. This creates eccentric annular region. For these reasons it is necessary to study flow of non-Newtonian fluid in annular region subjected to peristalis.

Shapiro *et al*. [17] has modelled peristaltic flow mathematically assuming small Reynolds number flow and a long wavelength approximation. Latham [6] has tried to model and understand peristalsis. A study on Power-law fluid under peristalsis in assymetric tube conducted by Raju and Devanathan [13].

Shapiro *et al*. [17] have used wave frame but same study is conducted by Fung and Yih [2] in laboratory frame. Radhakrishnamacharya [12] has considered Power law fluid and Srivastava and Srivastava [18] have considered Casson fluid. Usha and Rao [19], and Eytan and Elad [1] have studied peristaltic flow in asymmetric channel with reference to uterine fluid flow. Mishra and Rao [9] have studied the effect of different amplitudes and different phases on asymmetric geometry to understand peristaltic flow. A two layered model was considered by Mishra and Pandey [10], in which inner layer was Casson fluid and outer Newtonian fluid layer subjected to peristaltic flow. Vajravelu *et al*. [20] considered Herschel Buckley fluid model. Pandey and Chaube [11] have investigated wall properties during peristaltic flow considering couple stress fluid. Mekheimer and Al-Arabi [7] have considered peristaltic transport under magnetic effect with non-linearity.

Hayat and Hina [3] have studied flow of a non-Newtonian fluid flow subjected to peristalsis and have analysed the effect of wall properties. Analytical study of flow of Power-law fluid under peristalsis was investigated by Sadeghi and Talab [16]. Kumar and Kavitha [5] have studied the slip effects on peristaltic flow in a non-uniform tube. Mekheimer *et al*. [8] have analysed peristaltic flow between eccentric cylinders and an analytical solution obtained by perturbation method. Rashmi *et al*. [15] have studied the peristaltic flow in doubly connected region considering the couple stress fluid. Ramrao *et al*. [14] have modelled the process of flow of Prandtl fluid subjected to peristalsis. Investigation of Prandtl fluid with heat transfer with respect to oesophagus has been carried out by Indira *et al*. [4].

In most of the studies above either symmetric or asymmetric tube is considered with flow of Newtonian and non-Newtonian fluid or concentric annulus is used. An attempt is made in the present study to analyse flow of Couple-Stress fluid in an annular region created by eccentrically placed cylinders under peristaltic motion. Analytical solution by perturbation and Frobenius method or used foe getting velocity, pressure and rate of flow.

2. Mathematical Formulation

A doubly connected region created by placing two cylindrical tubes eccentrically is considered. A couple stress fluid is assumed to be under peristaltic motion in the annular region. The physical configuration is as shown in Figure 1.

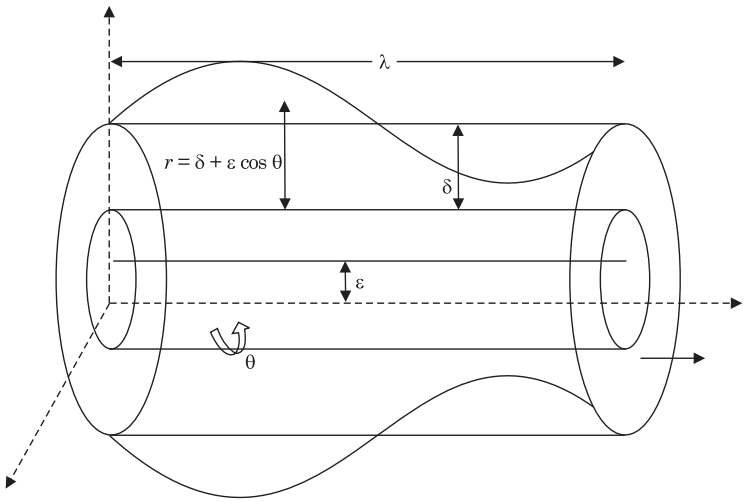

Figure 1. Physical configuration

The governing equations in the absence of body forces in vector form are given by,

$$\nabla \cdot \vec{q} = 0, \tag{2.1}$$

$$\rho\left[\frac{\partial \vec{q}}{\partial t} + (\vec{q}\cdot\nabla)\vec{q}\right] = -\nabla p + \mu\nabla^2\vec{q} - \eta\nabla^4\vec{q}. \tag{2.2}$$

A siusoidal wave propagates on the outer wall and inner being rigid. $r_1 = \delta + \epsilon\cos\theta$ is the radius of inner cylinder and $r_2 = a + b\cos\left[\frac{2\pi}{\lambda}(z-ct)\right]$ is the radius of the outer cylinder.

The velocity $\vec{q} = (u,v,w)$ in r,θ,z directions.

The boundary conditions are given by,

$$\vec{q} = 0 \text{ and } \nabla^2\vec{q} = 0 \text{ on } r = r_2 \tag{2.3}$$

and

$$\vec{q} = (v,0,0) \text{ and } \nabla^2\vec{q} = 0 \text{ on } r = r_1. \tag{2.4}$$

Non-dimensionalising the above governing equations and boundary conditions using the quantities,

$$p^* = \frac{a^2}{\mu c\lambda}p,\ \theta^* = \theta,\ t^* = \frac{c}{\lambda}t,\ (u,v,w)^* = \frac{u,v,w}{c},\ Re = \frac{\rho ca}{\mu},\ r_1^* = \frac{r_1}{a},\ r_2^* = \frac{r_2}{a},$$

$$\delta^* = \frac{\delta}{a},\ \epsilon^* = \frac{\epsilon}{a},\ \delta_0 = \frac{a}{\lambda},\ z^* = \frac{z}{\lambda},\ \phi = \frac{b}{a},$$

where ϵ — eccentricity, δ_0 — wave number, ϕ — amplitude ratio, and Re — Reynolds number.

Neglecting the asterisks and applying the low Reynolds number flow and long wave approximations, the governing equations become:

$$-\alpha^2\frac{dp}{dz} = \nabla^4 u - \alpha^2\nabla^2 u\,. \tag{2.5}$$

The velocity $u(r,\theta)$ is assumed as,

$$u = u_0(r) + \epsilon \cos\theta u_1(r) + \cdots . \tag{2.6}$$

Substituting equation (2.6) in the equation (2.5), we get the following equations by equating the different powers of ϵ:

Equations for ϵ^0,

$$\left[\frac{1}{r}\frac{\partial}{\partial r}\left(r\frac{\partial}{\partial r}\right)\right]^2 u_0 - \alpha^2\left[\frac{1}{r}\frac{\partial}{\partial r}\left(r\frac{\partial}{\partial r}\right)\right]u_0 = -\alpha^2\frac{dp}{dz}; \tag{2.7}$$

equations of order ϵ^1,

$$\left[\frac{1}{r}\frac{\partial}{\partial r}\left(r\frac{\partial}{\partial r}\right)+\frac{1}{r^2}\frac{\partial^2}{\partial\theta^2}\right]^2(u_1\cos\theta) - \alpha^2\left[\frac{1}{r}\frac{\partial}{\partial r}\left(r\frac{\partial}{\partial r}\right)+\frac{1}{r^2}\frac{\partial^2}{\partial\theta^2}\right](u_1\cos\theta) = 0 \tag{2.8}$$

subject to

$$u_0 = v \ \text{ on } \ r = r_1, \tag{2.9}$$

$$u_0 = 0 \ \text{ on } \ r = r_2, \tag{2.10}$$

$$u_1 = -\frac{\partial u_0}{\partial r} \ \text{ on } \ r = r_1, \tag{2.11}$$

$$u_1 = 0 \ \text{ on } \ r = r_2, \tag{2.12}$$

and vanishing couple-stresses at the boundary,

$$\nabla^2 u_0 = 0 \ \text{ and } \ \nabla^2 u_1 = 0 \ \text{ on } \ r = r_1 \ \text{ and } \ r = r_2. \tag{2.13}$$

2.1 Solution of Zeroth Order Component of Velocity

Let $\frac{1}{r}\frac{\partial}{\partial r}\left[r\frac{\partial u_0}{\partial r}\right] = U_0$, then the equation (2.2) becomes,

$$\frac{\partial^2 U_0}{\partial r^2} + \frac{1}{r}\frac{\partial U_0}{\partial r} - \alpha^2 U_0 = -\alpha^2\frac{dp}{dz}, \tag{2.14}$$

subjected to the boundary conditions,

$$U_0 = 0 \ \text{ on } \ r = r_1 \ \text{ and } \ r = r_2. \tag{2.15}$$

The above equation is a Bessel equation whose solution can be written as,

$$U_0 = AI_0(\alpha r) + BK_0(\alpha r) + \frac{dp}{dz}. \tag{2.16}$$

Using boundary conditions $U_0 = 0$ on $r = r_1$ and $r = r_2$, we get the constants as,

$$A = -\frac{dp}{dz}a_1 \ \text{ and } \ B = -\frac{dp}{dz}a_2. \tag{2.17}$$

Therefore,

$$U_0 = \frac{dp}{dz}[a_1 I_0(\alpha r) + a_2 K_0(\alpha r) + 1], \tag{2.18}$$

where $U_0 = \frac{1}{r}\frac{\partial}{\partial r}\left[r\frac{\partial u_0}{\partial r}\right]$.

Therefore,

$$\frac{1}{r}\frac{\partial}{\partial r}\left[r\frac{\partial u_0}{\partial r}\right] = \frac{dp}{dz}[a_1 I_0(\alpha r) + a_2 K_0(\alpha r) + 1]. \tag{2.19}$$

Integrating twice, we get

$$u_0 = \frac{dp}{dz}\left[\frac{r^2}{4} + \frac{a_1}{\alpha^2}I_0(\alpha r) + \frac{a_2}{\alpha^2}K_0(\alpha r)\right] + C\log r + D\,. \tag{2.20}$$

Using boundary conditions $U_0 = V$ on $r = r_1$ and $U_0 = 0$ on $r = r_2$, we get

$$C = -\frac{dp}{dz}c + \frac{V}{\log\frac{r_1}{r_2}} \tag{2.21}$$

and

$$D = -\frac{dp}{dz}\left[\frac{f(r_1)\log r_2 - f(r_2)\log r_1}{\log\frac{r_1}{r_2}} - V\frac{\log r_2}{\log\frac{r_2}{r_1}}\right]. \tag{2.22}$$

Substituting the constants the zeroth component of axial velocity is given by,

$$\begin{aligned} u_0(r) = &-\frac{dp}{dz}\left[\frac{f(r_1)-f(r_2)}{\log\frac{r_1}{r_2}}\log r + \frac{f(r_1)\log r_2 - f(r_2)\log r_1}{\log\frac{r_1}{r_2}} + \frac{a_1}{r^2}I_0(\alpha r) + \frac{a_2}{r^2}K_0(\alpha r) - \frac{r^2}{2}\right] \\ &+ \frac{V}{\log\frac{r_1}{r_2}}[\log r - \log r_2]. \end{aligned} \tag{2.23}$$

2.2 Solution of First Order Component of Velocity

The reduced form of equation (2.8) is,

$$\frac{\partial^4 u_1}{\partial r^4} + \frac{2}{r}\frac{\partial^3 u_1}{\partial r^3} - \frac{3}{r^2}\frac{\partial^2 u_1}{\partial r^2} + \frac{3}{r^3}\frac{\partial^2 u_1}{\partial r} - \frac{3}{r^4}u_1 - \alpha^2\left[\frac{\partial^2 u_1}{\partial r^2} + \frac{1}{r}\frac{\partial^2 u_1}{\partial r} - \frac{1}{r^2}u_1\right] = 0. \tag{2.24}$$

Solving the above equation using Frobenious method subject to the conditions given in equation (2.11) to equation (2.13), the solution takes the form:

$$u_1(r) = c_1\phi_1(r) + c_2\phi_2(r) + c_3\phi_3(r) + c_4\phi_4(r), \tag{2.25}$$

where

$$\phi_1(r) = 1 - \frac{\alpha^2}{4}r^2 + \sum_{n=2}^{\infty} G(n)r^{2n+1},$$

$$\phi_2(r) = y_1(r)\log r + 1 - \frac{\alpha^2}{4}r^2 + \sum_{k=2}^{\infty} G(n)\chi_1(n)r^{2n+1},$$

$$\phi_3(r) = y_1(r)\{(\log r)^2 + 2\log r\} + 1 - \frac{\alpha^2}{4}r^2 + \sum_{n=2}^{\infty} G(n)\{\chi_1^2(n) + \chi_2(n)\}r^{2n+1},$$

$$\begin{aligned} \phi_4(r) = {} & y_1(r)\{(\log r)^3 + 3(\log r)^2 + 3\log r\} + 1 - \frac{\alpha^2}{4}r^2 \\ & + 3\log r\sum_{n=2}^{\infty} G(n)\{\chi_1^2(n) + \chi_2(n)\}r^{2n+1} + 1 - \frac{5\alpha^2}{4}r^2 \\ & + \sum_{n=2}^{\infty} G(n)\{\chi_1^3(n) + \chi_2(n) + 3\chi_1(n)\chi_2(n)\}r^{2n+1}. \end{aligned}$$

The axial velocity will be given by

$$u(r) = u_0(r) + \epsilon\cos\theta u_1(r). \tag{2.26}$$

The rate of flow rate is given by

$$Q(z,t) = \int_{r_1}^{r_2} ru\,dr. \tag{2.27}$$

The pressure gradient is given by

$$\frac{dp}{dz} = \frac{Q - 2\pi V\Gamma_3 + \Gamma_4}{-2\pi\Gamma_1 + \epsilon\cos\theta\Gamma_2}, \tag{2.28}$$

where $Q(z)$ is considered as $Q = \bar{Q} + r_1^2 - \{1 + \frac{\phi^2}{2}\}$ following Shapiro *et al*. [17].
Pressure difference is,

$$\Delta p = \int_0^1 \frac{dp}{dz}dz, \tag{2.29}$$

and the frictional forces on inner and outer tube are given by,

$$F_i(t) = -\int_0^1 r_1^2 \frac{dp}{dz}dz \tag{2.30}$$

and

$$F_0(t) = -\int_0^1 r_2^2 \frac{dp}{dz}dz. \tag{2.31}$$

3. Results and Discussion

If endoscope or a catheter is inserted into oesophagus an eccentric annular region is created. The food bolus has to travel through oesophagus due to wavy motion of walls created by swallowing. Hence, this is modelled as eccentric annular flow of couple-stress fluid under peristaltic motion and studied in the current worl. Perturbation technique is applied with eccentricity as parameter, velocity, rate of flow and pressure gradient are obtained. The results are grpahically depicted.

The flow parameters are analysed graphically for the effects of variation in couple-stress parameter α, eccentricity ϵ and amplitude ratio. Figures 2-6 show velocity profile and Figures 7-13 show pressure gradient for different parameter.

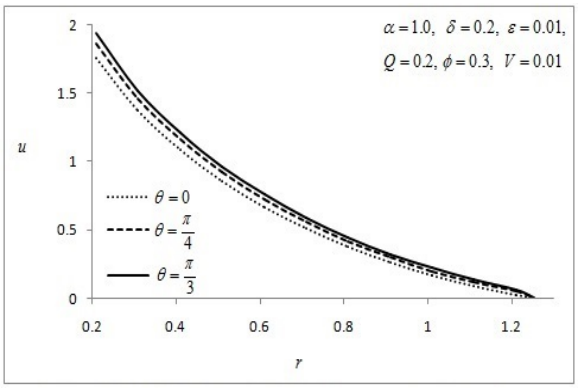

Figure 2. Radial velocity profile for different angular position θ

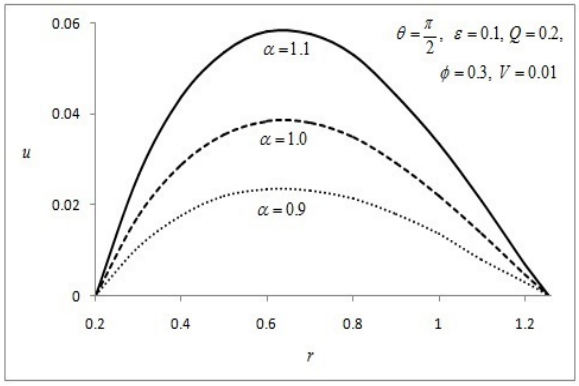

Figure 3. Radial velocity profile for different couple stress parameter α

Figures 3 and 5 show velocity $u(r) = u_0 + \epsilon\cos\theta u_1$ for different values of θ. As θ increases from 0° to 60° there is a slight decrement in the velocity. At $\theta = 90°$, the effect of ϵ will be absent as $\cos\theta$ becomes zero and $u(r) = u_0(r)$ will be a function of r only. Velocity shows parabolic profile,

this is shown in Figure 3. The effect of α is also shown in figure. α is inversely proportional to spin of the particles and as $\alpha \to \infty$, the fluid becomes Newtonian. As α increases, there is a significant increase in velocity. Least value of α corresponds to maximum spin of suspended particles. Hence as α decreases, the resistance to flow increases and velocity decreases provided volume flow rate is maintained constant.

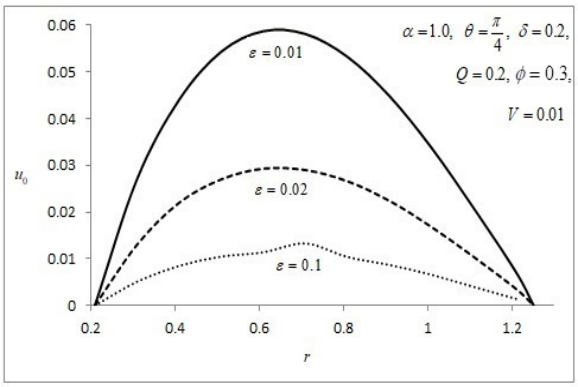

Figure 4. Radial velocity profile for different eccentricty ϵ

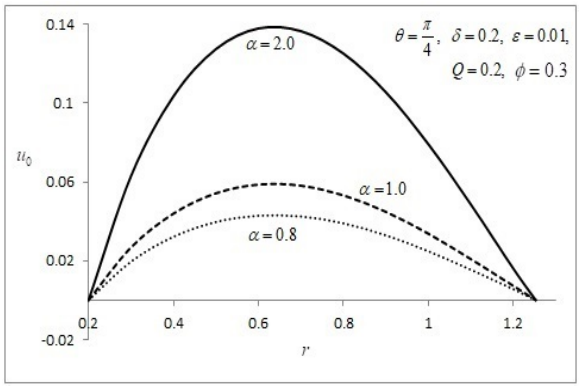

Figure 5. Radial velocity profile for different couple stress parameter α

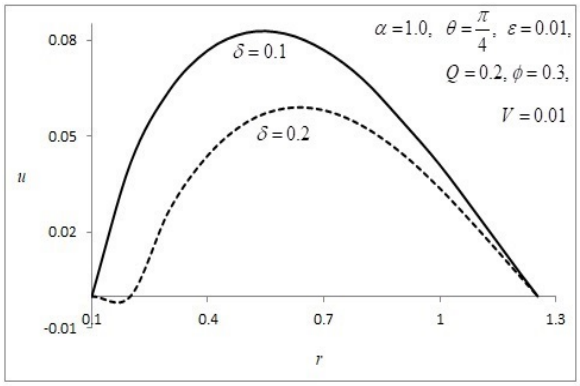

Figure 6. Radial velocity profile for different inner tube radius δ

Figures 4 and 6 show the influence of variation in radius of inner tube δ and eccenticity ϵ. As ϵ increases, velocity decrease for a given constant rate of flow due to increase in available area of cross section. As inner tube radius increases, the area of cross section for the flow will reduce and hence there is a reduction in velocity. This result is due to the fact that volume flow rate is maintained constant.

Figure 5 shows the effect of couple stress parameter on zeroth component of velocity which shows the same effect as in case of Figure 3 where $u(r) = u_0 + \epsilon \cos\theta u_1$ is plotted. The zero component of velocity u_0 is not affected by ϵ, the eccentricity hence is very close to the results of concentric annulus.

Figures 7-12 show pressure gradient plotted against axial coordinate z or time t (non dimensional). Effect of various parameters are assessed in each figure.

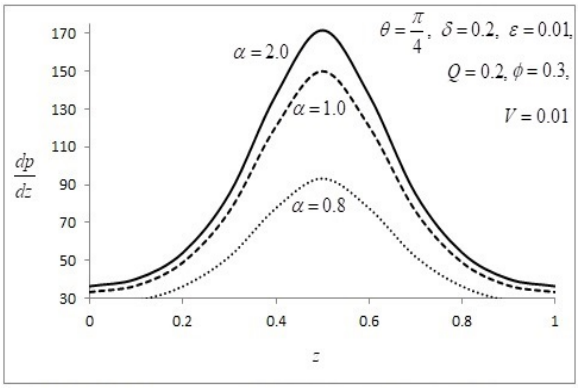

Figure 7. Axial pressure gradient for different couple stress parameter α

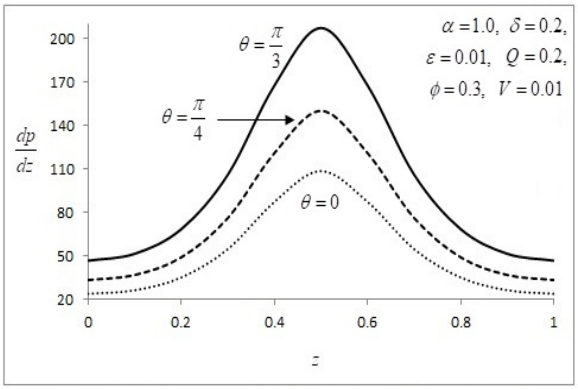

Figure 8. Axial pressure gradient for different azimuthal coefficient θ

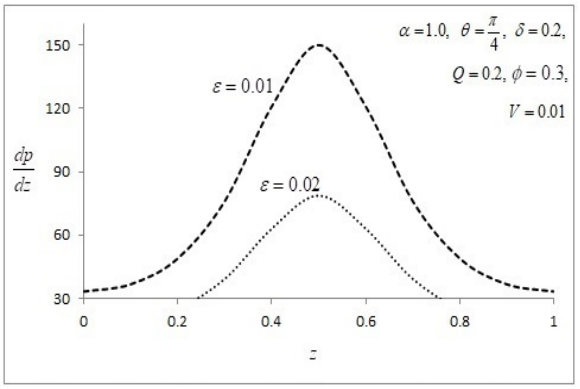

Figure 9. Axial pressure for different eccentricty ϵ

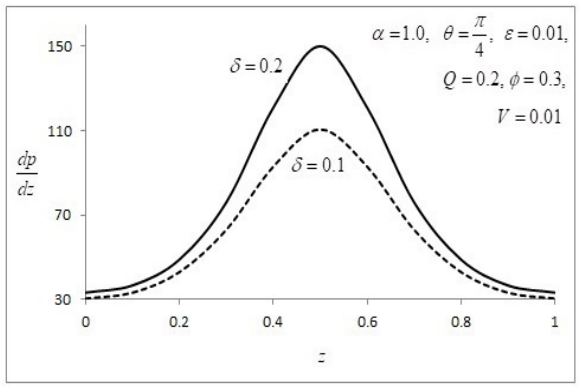

Figure 10. Axial pressure gradient for different inner tube radius δ

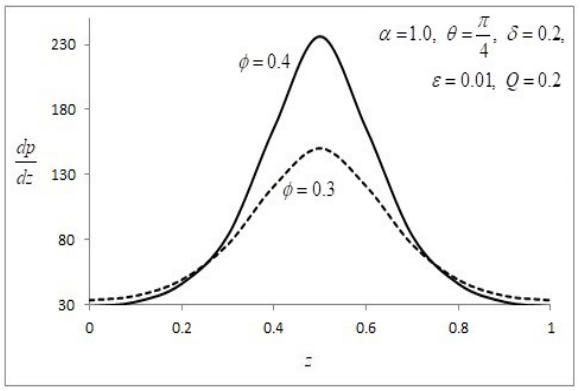

Figure 11. Axial pressure gradient for different amplitude ratio ϕ

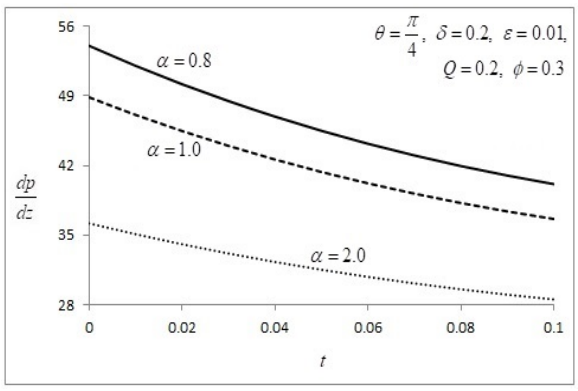

Figure 12. Axial pressure gradient for different couple stress parameter α

Figure 7 shows effect of couple stress parameter on pressure gradient. Since volume flow rate is maintained constant as velocity decreases with decrease in couple stress parameter, the pressure gradient increases in order to maintain constant Q. α is inversely proportional to spin of the particles, hence as α increases, the spin decreases indicating less amount of suspended particles present. Figure 8 shows effect of θ on the pressure gradient. It shows inclination of radial line to the axis and indicates different annular position in the annular region. As θ

changes, there will be a change in pressure gradient showing the effect of eccentricity. As θ changes from 0 to 60°, there is increase in pressure gradient. On the axis pressure is minimum and as we move towards the vertical axis $\theta = 90°$ pressure increases. As eccentricity increases, the pressure decreases due to increases in area of cross section available for flow. Since Q, the rate of flow is maintained constant and there is slight increase in velocity, the decrease in pressure gradient is evident.

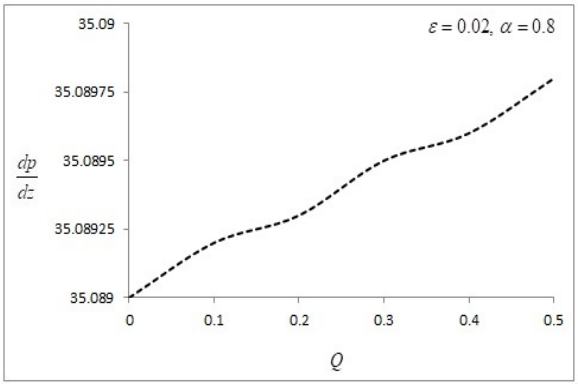

Figure 13. Axial pressure gradient vs rate of flow

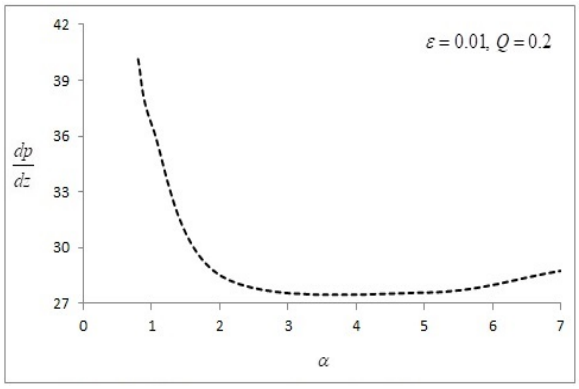

Figure 14. Axial pressure gradient vs couple stress parameter α

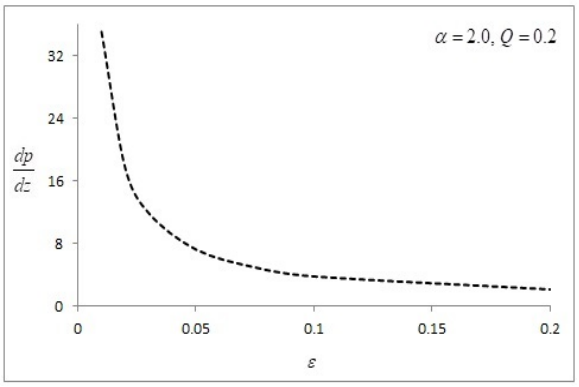

Figure 15. Axial pressure gradient vs rate of flow

Figure 9 shows the effect of eccentricity on pressure gradient and as increased eccentricity facilitates higher area of cross-section for the flow, there will be a smaller wave form for the pressure and effect is very significant. Figure 10 shows, effect of inner tube radius. As δ increases, it results in reduction of cross sectional area and hence there is increase of pressure in order to maintain constant flow rate. Figure 11 shows effect of amplitude ratio ϕ. Initially pressure gradient decreases but in the middle of the tube it increases and later it decreases as ϕ increases. This is due to the wave form motion of the wall whose amplitude define ϕ. Figure 12 shows variation of pressure gradient with respect to non dimensional time. The pressure gradient decreases sharply with time. The graphs also show the effect of stress parameter α on $\frac{\partial p}{\partial z}$.

Figure 13 shows effect of increase of Q on $\frac{\partial p}{\partial z}$. As Q increases, there is a very slight change in $\frac{\partial p}{\partial z}$. Figure 14 shows variation of eccentricity on $\frac{\partial p}{\partial z}$. As ϵ increases, the pressure gradient

decreases significantly. Figure 15 shows effect of couple stress parameter. Pressure gradient decreases significantly with increase in α which tends to show Newtonian nature.

4. Conclusions

The study given an insight of flow characteristics of peristaltic flow in an eccentric annular region created by placing two cylinders one inside the other. This geometry helps us to understand the flow in an artery in presence of catheter or endoscope present inside the digestive or urinary system. The results highlight the fact that non-Newtonian nature increases the pressure gardient and decreases the velocity. The eccentricity in the geometry is a natural effect of restrictions on pressure and mass flow rate in the biological system. As there is a need for blood flow rate to be maintained in the body, any henderence in the flow results in increase of pressure gradient. This naturally creates a situation where excess pressure has to be reduced and the catheter or endoscope will be pushed to the wall creating more area for the flow, hence creating eccentric annular region. This fact is dimensionalised from the result. As couple stress parameter $\alpha \to \infty$, the results reduces to that of Newtonian fluid.

Acknowledgments

The authors extend their special thanks the management of Nitte Meenakshi Institute of Technology, Bengaluru and Reva University, Bengaluru for their cooperation in bringing out of this work.

Appendix

$$r_1 = \delta + \epsilon\cos\theta,$$

$$r_2 = 1 + \cos[2\pi(z-t)],$$

$$a_1 = \frac{k_0(\alpha r_2) - k_0(\alpha r_1)}{I_0(\alpha r_2)k_0(\alpha r_1) - k_0(\alpha r_2)I_0(\alpha r_1)},$$

$$a_2 = \frac{I_0(\alpha r_2) - I_0(\alpha r_1)}{I_0(\alpha r_1)k_0(\alpha r_2) - k_0(\alpha r_1)I_0(\alpha r_2)},$$

$$f(r) = \frac{r^2}{4} + \frac{a_1}{\alpha^2}I_0(\alpha r) + \frac{a_2}{\alpha^2}k_0(\alpha r),$$

$$c = \frac{f(r_1) - f(r_2)}{\log\frac{r_1}{r_2}},$$

$$d = f(r_1) - c\log r_1,$$

$$g(r) = c\frac{r^2}{4}(2\log r - 1) - \frac{a_1}{\alpha^2}rI_1(\alpha r) - \frac{a_2}{\alpha^2}rk_1(\alpha r) - \frac{r^4}{16} + \alpha\frac{r^2}{2},$$

$$L_i = \phi_i' + \phi_i'',$$

$$S_1(r) = \frac{c}{r} + \frac{a_1}{\alpha}I_0'(r) + \frac{a_2}{\alpha}k_0'(r),$$

$$S_2(r) = \frac{1}{r\log\frac{r_1}{r_2}},$$

$$T_1 = L_2(r_1)L_1(r_2) - L_2(r_2)L_1(r_1),$$
$$T_2 = L_3(r_1)L_1(r_2) - L_3(r_2)L_1(r_1),$$
$$T_3 = L_4(r_1)L_1(r_2) - L_4(r_2)L_1(r_1),$$
$$Y_1 = \phi_1(r_1)L_2(r_1) - L_1(r_1)\phi_2(r_1),$$
$$Y_2 = \phi_1(r_1)L_3(r_1) - L_1(r_1)\phi_3(r_1),$$
$$Y_3 = \phi_1(r_1)L_4(r_1) - L_1(r_1)\phi_4(r_1),$$
$$X_1 = \phi_1(r_2)L_2(r_1) - L_1(r_1)\phi_2(r_2),$$
$$X_2 = \phi_1(r_2)L_3(r_1) - L_1(r_1)\phi_3(r_2),$$
$$X_3 = \phi_1(r_2)L_4(r_1) - L_1(r_1)\phi_4(r_2),$$
$$\beta_1 = T_2Y_1 - Y_2T_1,$$
$$\beta_2 = T_3Y_1 - Y_3T_1,$$
$$\beta_3 = T_2X_1 - X_2L_2(r_2),$$
$$\beta_4 = T_3X_2 - X_3L_2(r_2),$$
$$\beta_5 = Y_3\beta_3 - Y_2\beta_4,$$
$$c_1 = \frac{c_4L_4(r_1) + c_3L_3(r_1) + c_2L_2(r_1)}{L_1(r_1)},$$
$$c_2 = -\frac{(c_4T_3-)}{T_1},$$
$$c_3 = \frac{L_1(r_1)T_1 - L_1(r_1)T_1X_2}{Y_2},$$
$$c_4 = \frac{\phi_1(r_1)T_1X_2}{\beta_5},$$
$$G(n) = \frac{-\alpha^{2n}(2n-1)!(2n-3)!}{2^{6n}(n!)^2(n-2)!\{(n-1)!\}^2},$$
$$\chi_1(n) = \sum_{i=1}^{n-1}\frac{1}{2n-1} + \frac{2}{2i-1},$$
$$\chi_2(n) = \sum_{i=1}^{n-1}\frac{1}{2n-1} + \frac{2}{(2i-1)^2},$$
$$\gamma_1 = \int_{r_1}^{r_2}[c_1\phi_1(r) + c_2\phi_2(r) + c_3\phi_3(r) + c_4\phi_4(r)]rdr,$$
$$\Gamma_1 = g(r_1) - g(r_2),$$
$$\Gamma_2 = 2\pi S_1(r_1)\gamma_1,$$
$$\Gamma_3 = \frac{r_2^2\left(2\log\frac{r_2}{r_1} - 1\right) + r_1^2}{4\log\frac{r_1}{r_2}},$$
$$\Gamma_4 = 2\pi\phi_2(r_1)\gamma_1.$$

Competing Interests

The authors declare that they have no competing interests.

Authors' Contributions

All the authors contributed significantly in writing this article. The authors read and approved the final manuscript.

References

[1] O. Eytan and D. Elad, Analysis of intra-uterine fluid motion induced by uterine contractions, *Bulletin of Mathematical Biology* **61** (1999), 221 – 238, DOI: 10.1006/bulm.1998.0069.

[2] Y. C. Fung and C. S. Yih, Peristaltic transport, *Journal of Applied Mechanics* **85** (1968), 669 – 675, DOI: 10.1115/1.3601290.

[3] T. Hayat and S. Hina, The influence of wall properties on the MHD peristaltic flow of a Maxwell fluid with heat and mass transfer, *Nonlinear Analysis: Real World Applications* **11**(4) (2010), 3155 – 3169, DOI: 10.1016/j.nonrwa.2009.11.010.

[4] R. Indira, K. R. Sreegowrav and P. A. Dinesh, Effect of heat transfer on peristaltic flow of couple stress fluid in oesophagus, *International Journal of Pure and Applied Mathematics* **120**(6) (2018), 1321 – 1335, URL: https://www.acadpubl.eu/hub/2018-120-6/9/901.pdf.

[5] K. T. Kumar and A. Kavitha, The influence of slip effects on peristaltic transport of a Rabinowitsch fluid model in a non uniform tube, *IOP Conference Series: Materials Science and Engineering* **263** (2017), 062004, DOI: 10.1088/1757-899X/263/6/062004.

[6] T. W. Latham, *Fluid Motions in a Peristaltic Pump*, M.S. Thesis, Massachusetts Institute of Technology, Cambridge, MA, USA (1966), URL: https://dspace.mit.edu/handle/1721.1/17282.

[7] K. S. Mekheimer and T. H. Al-Arabi, Nonlinear peristaltic transport of MHD flow through a porous medium, *International Journal of Mathematics and Mathematical Sciences* **2003** (2003), Article ID 537431, 20 pages, DOI: 10.1155/S0161171203008056.

[8] Kh. S. Mekheimer, Y. A. Elmaboud and A. I. Abdellateef, Peristaltic transport through eccentric cylinders: mathematical model, *Applied Bionics and Biomechanics* **10** (2013), Article ID 902097, 9 pages, DOI: 10.3233/ABB-2012-0071.

[9] M. Mishra and A. R. Rao, Peristaltic transport of a Newtonian fluid in an asymmetric channel, *Zeitschrift für angewandte Mathematik und Physik ZAMP* **54** (2003), 532 – 550, DOI: 10.1007/s00033-003-1070-7.

[10] J. C. Misra and S. K. Pandey, Peristaltic transport of blood in small vessels: study of a mathematical model, *Computers & Mathematics with Applications* **43**(8-9) (2002), 1183 – 1193, DOI: 10.1016/S0898-1221(02)80022-0.

[11] S. K. Pandey and M. K. Chaube, Study of wall properties on peristaltic transport of a couple stress fluid, *Meccanica* **46** (2011), 1319 – 1330, DOI: 10.1007/s11012-010-9387-8.

[12] G. Radhakrishnamacharya, Long wavelength approximation to peristaltic motion of a power law fluid, *Rheologica Acta* **21** (1982), 30 – 35, DOI: 10.1007/BF01520703.

[13] K. K. Raju and R. Devanathan, Peristaltic motion of a non-Newtonian fluid, *Rheologica Acta* **11**(2) (1972), 170 – 178, DOI: 10.1007/BF01993016.

[14] I. Ramarao, P. N. Basavaraju and J. Seethappa, Peristaltic flow and heat transfer through a prandtl fluid in vertical annulus, in: *Recent Advances in Mechanical Engineering*, S. Narendranth, P. G. Mukunda and U.K. Saha (editors), Lecture Notes in Mechanical Engineering, 173 – 186, Springer, Singapore (2022), DOI: 10.1007/978-981-19-1388-4_16

[15] K. R. Rashmi, I. Ramarao and S. Jagadeesha, Peristaltic flow of couple-stress fluid in doubly connected region with reference to endoscope, *Palestine Journal of Mathematics* **10** (2021), 1 – 5, URL: https://pjm.ppu.edu/paper/829-peristaltic-flow-couple-stress-fluid-doubly-connected-region-reference-endoscope.

[16] K. Sadeghi and H. J. Talab, Analytical investigation of peristaltic transport of power law fluid through a tube, *Journal of Applied Mechanical Engineering* **3**(1) (2014), Article ID 1000136, 6 pages, DOI: 10.4172/2168-9873.1000136.

[17] A. H. Shapiro, M. Y. Jaffrin and S. L. Weinberg, Peristaltic pumping with long wavelengths at low Reynolds number, *Journal of Fluid Mechanics* **37**(4) (1969), 799 – 825, DOI: 10.1017/S0022112069000899.

[18] L. M. Srivastava and V. P. Srivastava, Peristaltic transport of blood: Casson model—II, *Journal of Biomechanics* **17**(11) (1984), 821 – 829, DOI: 10.1016/0021-9290(84)90140-4.

[19] S. Usha and A. R. Rao, Peristaltic transport of two-layered power-law fluids, *Journal of Biomechanical Engineering* **119**(4) (1997), 483 – 488, DOI: 10.1115/1.2798297.

[20] K. Vajravelu, S. Sreenadh and V. R. Babu, Peristaltic pumping of a Herschel–Bulkley fluid in a channel, *Applied Mathematics and Computation* **169**(1) (2005), 726 – 735, DOI: 10.1016/j.amc.2004.09.063.